

# Spin manipulation in a double quantum-dot–quantum-wire coupled system

S. Sasaki<sup>a)</sup>

*NTT Basic Research Laboratories, NTT Corporation, Atsugi, Kanagawa 243-0198, Japan*

S. Kang

*Institute of Physics, University of Tsukuba, Tsukuba, Ibaraki 305-8571, Japan  
and CREST-JST, Honmachi, Kawaguchi, Saitama 331-0012, Japan*

K. Kitagawa

*Faculty of Science, Tokyo University of Science, Kagurazaka, Tokyo 162-8601, Japan  
and CREST-JST, Honmachi, Kawaguchi, Saitama 331-0012, Japan*

M. Yamaguchi

*NTT Basic Research Laboratories, NTT Corporation, Atsugi, Kanagawa 243-0198, Japan  
and CREST-JST, Honmachi, Kawaguchi, Saitama 331-0012, Japan*

S. Miyashita and T. Maruyama

*NTT Advanced Technology Corporation, Atsugi, Kanagawa 243-0198, Japan*

H. Tamura and T. Akazaki

*NTT Basic Research Laboratories, NTT Corporation, Atsugi, Kanagawa 243-0198, Japan  
and CREST-JST, Honmachi, Kawaguchi, Saitama 331-0012, Japan*

Y. Hirayama

*NTT Basic Research Laboratories, NTT Corporation, Atsugi, Kanagawa 243-0198, Japan  
and SORST-JST, Honmachi, Kawaguchi, Saitama 331-0012, Japan*

H. Takayanagi

*NTT Basic Research Laboratories, NTT Corporation, Atsugi, Kanagawa 243-0198, Japan,  
Faculty of Science, Tokyo University of Science, Kagurazaka, Tokyo 162-8601, Japan,  
and CREST-JST, Honmachi, Kawaguchi, Saitama 331-0012, Japan*

(Received 17 January 2006; accepted 16 May 2006; published 25 July 2006)

We have studied spin correlation in a double quantum-dot–quantum-wire coupled device revealed in low-temperature transport characteristics. We demonstrate nonlocal control of the Kondo effect in one dot by manipulating the spin states of the other. The modulation of the local density of states in the wire region due to the Fano-Kondo antiresonance and the Ruderman-Kittel-Kasuya-Yoshida exchange interaction are the two possible mechanisms underlying the observed features. When the dot states are indirectly probed in the side-coupled geometry, double suppression of the wire conductance is observed due to the Fano-Kondo antiresonance involving both dots. © 2006 American Vacuum Society. [DOI: 10.1116/1.2218866]

## I. INTRODUCTION

Recent advances in the fabrication of semiconductor nanostructures have opened up possibilities to investigate various quantum correlation effects. A quantum dot (QD) is an important building block for constructing functional devices since its electronic states are tunable by external parameters such as gate voltages and magnetic field. The QD behaves as a single magnetic impurity with spin  $S=1/2$  when it holds an odd number  $N$  of electrons. This magnetic aspect is clearly revealed in the Kondo effect, where the spin in the QD antiferromagnetically couples with another spin in the lead electrodes at low temperatures.<sup>1–6</sup> The Kondo effect manifests itself as an increase of the conductance at Coulomb blockade regions, and as a zero-bias peak in the differential conductance versus source-drain bias characteristics, which results from the coherent higher order tunneling. This is the case for the conventional geometry where the source

and drain electrodes are attached to both ends of the dot; i.e., the only current path is through the “magnetic impurity.”

When a QD is attached to the side of another quantum wire (QW), on the other hand, the Fano resonance is observed in the conductance of the QW due to an interference between a localized state of the QD and a continuum of the QW.<sup>7–9</sup> Moreover, in the odd electron number regions between two Fano resonances, the electrons in the QW experience enhanced scattering by the localized spin in the QD, or the Kondo “cloud” suppresses the QW conductance, which is referred to as the Fano-Kondo antiresonance.<sup>10–14</sup> By adding a second QD to this dot-wire coupled system, one can study the indirect correlation between two localized spins mediated by conduction electrons in the interceding QW, which is known as Ruderman-Kittel-Kasuya-Yoshida (RKKY) interaction.<sup>15–20</sup>

In this article, we present a transport measurement on two QDs coupled to the opposing sides of a quasi-one-dimensional QW.<sup>16</sup> This system offers the minimum interdot distance realizable in lateral mesoscopic devices, and is ad-

<sup>a)</sup>Electronic mail: satoshi@nttbl.jp

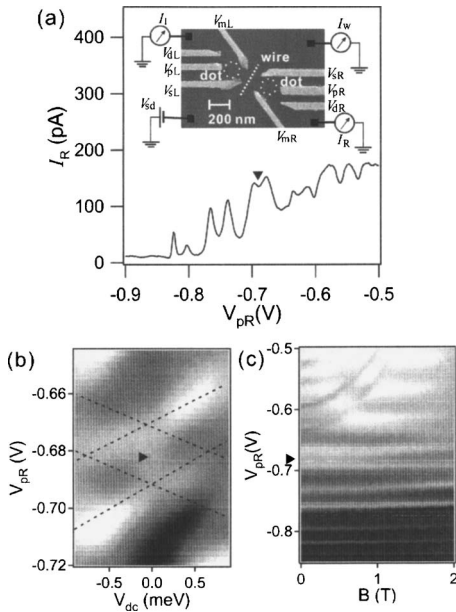


FIG. 1. (a) Current through the right QD,  $I_R$  in response to excitation source-drain voltage  $V_{sd}=3 \mu\text{V}$  ( $V_{dc}=0 \text{ V}$ ) as a function of  $V_{pR}$ . A solid triangle denotes a Kondo valley with an odd  $N_R$ . The left QD is not formed yet. The inset shows a scanning electron micrograph of the double QD-QW coupled device together with a schematic of the measurement setup. Dotted lines indicate the positions of the QDs and QW. (b) Gray-scale plot of the conductance through the right QD as a function of  $V_{dc}$  and  $V_{pR}$ . Black corresponds to  $15 \mu\text{S}$  and white to  $65 \mu\text{S}$ . Dotted lines denote edges of the Coulomb diamonds and a solid triangle denotes a Kondo ridge found in the odd  $N_R$  Coulomb blockade region. (c) Gray-scale plot of the conductance through the right QD as a function of magnetic field and  $V_{pR}$  ( $V_{pR}=0 \text{ V}$ ). Black corresponds to  $0 \text{ S}$  and white to  $70 \mu\text{S}$ . A solid triangle denotes the Kondo valley.

vantageous for studying the RKKY interaction, which decays on the length scale of the Fermi wavelength. We demonstrate nonlocal control of the Kondo effect in one dot by tuning the spin states of the other, which suggests the RKKY interaction as an underlying mechanism. We also discuss the Fano-Kondo antiresonance effect in the side-coupled geometry where the QD states are indirectly probed via the QW conductance.

## II. EXPERIMENT

The inset to Fig. 1(a) shows the double QD-QW coupled device fabricated by depositing Ti/Au Schottky gates on the surface of a GaAs/ $\text{Al}_x\text{Ga}_{1-x}\text{As}$  heterostructure. The two-dimensional electron gas (2DEG) is located  $90 \text{ nm}$  below the surface. Two QDs and a QW between them are formed (shown by dotted lines) by biasing the eight gates. To avoid the formation of another QD in the central QW region,  $V_{sR}$  and  $V_{sL}$  are biased more negatively than  $V_{mR}$  and  $V_{mL}$ . Transport measurement is performed with a standard lock-in technique at temperature of about  $100 \text{ mK}$  in a dilution refrigerator. The source-drain bias  $V_{sd}=V_{dc}+V_{ac}$ , where  $V_{dc}$  is a dc offset, and ac excitation (about  $13 \text{ Hz}$ )  $V_{ac}=3 \mu\text{V}$ . Magnetic field perpendicular to the 2DEG plane is applied mainly to reduce the tunnel coupling without electrostatic energy shift.

## III. RESULTS AND DISCUSSION

We begin by confirming the conventional Kondo effect in a single QD. We form only the right QD with  $V_{sR}=-1.35 \text{ V}$ ,  $V_{dR}=-0.39 \text{ V}$ , and  $V_{mR}=-0.45 \text{ V}$ , such that the tunnel coupling between the QD and the source lead and that between the QD and the drain lead are almost equal. Figure 1(a) shows the current through the right QD,  $I_R$ , as a function of  $V_{pR}$  (Coulomb oscillation characteristics) when the left QD is not formed yet. Pairs of Coulomb oscillation peaks are observed suggesting that the electron number in the right QD,  $N_R$ , is odd in the Coulomb blockade regions between paired peaks (at  $V_{pR}=-0.81, -0.75$ , and  $-0.69 \text{ V}$ ). The dot-lead tunnel coupling increases as  $V_{pR}$  increases because of the capacitive coupling between different gates. Then, the Kondo temperature increases, leading to the increased conductance in the odd  $N_R$  Coulomb blockade valleys for more positive  $V_{pR}$ . For instance, the conductance at the valley marked with a solid triangle is significantly enhanced due to the Kondo effect. Figure 1(b) shows Coulomb diamond characteristics where the conductance is plotted as a function of the source-drain voltage,  $V_{dc}$ , and the plunger gate voltage  $V_{pR}$ . The conductance is enhanced along  $V_{dc}=0$  only within the odd  $N_R$  diamond forming a ridge structure (solid triangle), which corroborates the Kondo effect.

Figure 1(c) shows magnetic field dependence of the Coulomb oscillation characteristics. The Kondo effect is suppressed owing to the Zeeman splitting and the reduced dot-lead tunnel coupling as magnetic field increases. Consequently, the conductance at the Kondo valley marked with a solid triangle gradually decreases. At the same time, the alternating high and low conductance regions are observed at more positive  $V_{pR}$  forming a pattern like a chessboard.<sup>21</sup> As magnetic field increases, rearrangement of electrons occurs between the outer orbital (the ground Landau level) and the inner orbital (the higher Landau level) within the fixed total  $N_R$  region. Since the outer orbital is coupled with the leads more strongly than the inner orbital, the Kondo effect occurs when the electron number in the *outer* orbital, rather than the *total* electron number, is odd, resulting in the observed chessboard pattern.

Next, we form another QD (the left QD) by biasing the other gates. The exit tunnel barrier of the left QD is completely pinched off such that the only current path is through the right QD. This is done to avoid a spurious mirror effect, which occurs in the presence of multiple current paths.<sup>22</sup> Figure 2(a) shows the gray-scale plot of the conductance through the right QD as a function of  $V_{pL}$  and  $V_{pR}$ . The gate voltage that controls the coupling of the left QD with the rest of the system,  $V_{sL}=-1.04 \text{ V}$ , is adjusted in the weak-coupling regime. The two dotted lines designate Coulomb oscillation peaks for the right QD, and the region between them is the same Kondo valley as the one marked with a triangle in Fig. 1. The position of the Coulomb oscillation peaks are shifted from that in Fig. 1 due to slightly different gate voltage conditions. A series of almost vertical ridges are observed as  $V_{pL}$  is swept. When the conductance through the QW is independently measured as a function of  $V_{pL}$  with the

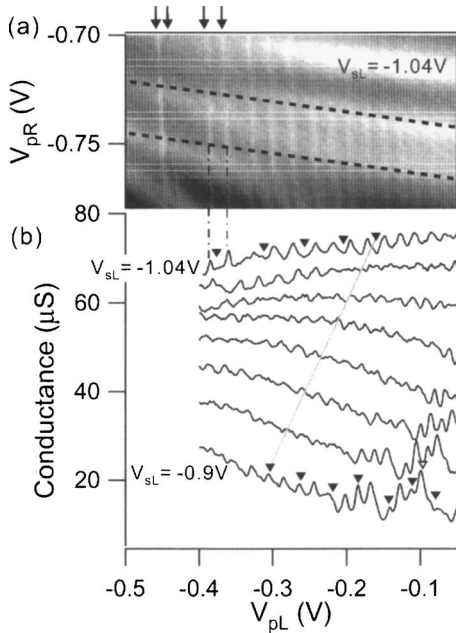


FIG. 2. (a) Gray-scale plot of the conductance through the right QD as a function of  $V_{pL}$  and  $V_{pR}$  in the weak-coupling regime with  $V_{sL} = -1.04$  V. Black corresponds to  $10 \mu\text{S}$  and white to  $42 \mu\text{S}$ . Dotted lines denote Coulomb oscillation peaks for the right QD and the region between the dotted lines correspond to odd  $N_R$ . Arrows on the upper horizontal axis mark two sets of spin-pair resonances. (b) Conductance profiles taken along the mid-Kondo valley of the right QD with the coupling gate voltage  $V_{sL}$  changed between  $-0.9$  and  $-1.04$  V in  $20$  mV steps.  $V_{pR}$  is simultaneously swept to trace the midvalley. For clarity, curves are offset vertically. The scales on the axes apply to the lowermost  $V_{sL} = -0.9$  V trace. The two dash-dotted lines denote spin-pair peaks. Odd  $N_L$  regions are marked with solid triangles, and one even  $N_L$  region on the  $V_{sL} = -0.9$  V trace is marked with an open triangle. A gray solid line connects the same  $N_L$  regions in  $V_{sL} = -0.9$  V and  $V_{sL} = -1.04$  V traces.

same gate voltage conditions, the Fano resonances associated with the left QD are observed as slightly asymmetric peaks.<sup>23</sup> Since these Fano resonances are almost in phase with the above ridges found in the right QD conductance, we assign the ridges to the resonances of the left QD states with the chemical potential of the lead. The ridges are not observed when  $V_{sL}$  is smaller than about  $-1.2$  V because the left QD is decoupled from the rest of the system. Please note that the four ridges marked with arrows form two sets of pairs, suggesting that up-spin and down-spin electrons consecutively occupy the same orbital state within the pair. Based on this spin-pair behavior, we deduce that narrow gaps within the pair correspond to the Coulomb blockade regions where the number of electrons in the left QD,  $N_L$ , is odd. Although the Kondo valley conductance is somewhat reduced from the original value at  $V_{pL} = 0$ , the Kondo effect still remains between the ridges. For the present weak-coupling condition, there is no noticeable difference in the conductance between even and odd  $N_L$  regions. Although no more ridges are observed at  $V_{pL} < -0.5$  V, this does not guarantee that  $N_L = 0$  there. In the case of the charge detection scheme, where the electrostatic energy shift caused by a change in  $N$  is measured by a nearby point contact, zero electron regime is commonly reached.<sup>24–26</sup> In our present measurement, on the

other hand, the resonance signal disappears if the tunnel coupling of the left QD is lost due to more negative  $V_{pL}$  even when  $N_L \neq 0$ .

Next, we increase the coupling of the left QD by increasing  $V_{sL}$ . Figure 2(b) shows the evolution of the conductance profiles taken along the mid-Kondo valley of the right QD when  $V_{sL}$  is changed from  $-1.04$  V (weak-coupling regime) to  $-0.9$  V (strong-coupling regime). The resonances associated with the left QD states appear as peaks in the weak-coupling regime. The spin-pair peaks and the odd  $N_L$  regions are marked with dash-dotted lines and solid triangles, respectively. We estimated the shift in  $V_{pL}$  of the resonance peaks in the weak-coupling regime in response to a slight shift in  $V_{sL}$  that does not affect the Fano line shape, and found that the electrostatic energy shift caused by  $V_{sL}$  is almost identical to that caused by  $V_{pL}$  in our device. Based on this, we found that the resonances appearing as conductance maxima in the weak-coupling regime change into minima in the strong-coupling regime, just as in the previous report by Sato *et al.*<sup>14</sup> The same odd  $N_L$  regions in the uppermost trace and lowermost one are connected with a gray solid line.

Figure 3(a) shows a plot similar to Fig. 2(a), but with  $V_{sL} = -0.9$  V, in the strong-coupling regime. Here, in contrast to Fig. 2(a), the resonances of the left QD states produce conductance minima. The intensity of the several conductance maxima corresponding to fixed  $N_L$  seems to alternate between  $V_{pL} = -130$  and  $-70$  mV. Here, the maxima at  $V_{pL} = -90$  mV correspond to the even  $N_L$  peak marked with an open triangle in Fig. 2(b), although the position is slightly shifted because of the different measurement time. As shown in Fig. 3(c), the zero-bias Kondo peak still remains in the  $dI_R/dV_{dc}$  vs  $V_{dc}$  characteristics. On the other hand, the conductance is smaller at two adjacent maxima with odd  $N_L$  (at  $V_{pL} = -102$  and  $-73$  mV), and no Kondo peak is found, as shown in Fig. 3(c). Thus, a nonlocal control of the Kondo effect in the right QD is realized by changing the number of electrons in the left QD.

When the Fano resonance involving the left QD modulates the conductance of the QW, it also indirectly modulates the dot current  $I_R$  since the QW acts as one lead for the right QD. As coupling of the left QD increases, the Fano-Kondo antiresonance suppresses the conductance at the odd  $N_L$  regions.<sup>14</sup> It is expected that the Fano resonance modulates the local density of states of the QW, as the enhanced zero-bias conductance shown in Fig. 3 in Ref. 8 suggests. Because  $T_K \propto \exp(-1/\rho J)$ , where  $\rho$  is the density of states and  $J$  is the coupling constant,<sup>27</sup>  $T_K$  decreases when  $\rho$  decreases. This may be one mechanism for the suppressed Kondo effect for the odd  $N_L$  cases because  $\rho$  is reduced by the Fano-Kondo effect compared to even  $N_L$ .

Another mechanism that could be responsible for the observed even-odd effect is the RKKY interaction. When both  $N_R$  and  $N_L$  are odd, the RKKY interaction couples two spins in the two QDs via interceding conduction electrons either ferromagnetically or antiferromagnetically depending on the distance between them. The effective interdot distance in our device is considered to be close to zero since they couple to

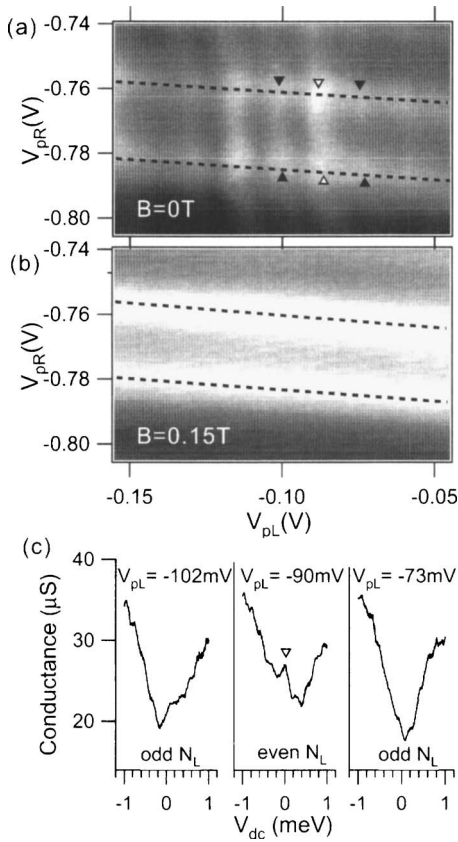


FIG. 3. (a) Gray-scale plot of the conductance through the right QD as a function of  $V_{sL}$  and  $V_{pR}$  with  $V_{sL} = -0.9$  V in the strong-coupling regime. Black corresponds to  $5 \mu S$  and white to  $35 \mu S$ . Dotted lines denote Coulomb oscillation peaks for the right QD and the region between the dotted lines correspond to odd  $N_R$  Kondo valley. The open and solid triangles denote even and odd  $N_L$  regions, respectively. (b) The same plot as (a) except  $B = 0.15$  T. (c)  $dI_R/dV_{dc}$  vs  $V_{dc}$  for odd  $N_L$  [ $V_{pL} = -102$  and  $-73$  mV, the solid triangles in (a)] and for even  $N_L$  [ $V_{pL} = -90$  mV, the open triangle in (a)].  $V_{pR}$  is fixed at  $-775$  mV in the middle of the odd  $N_R$  Coulomb blockade valley. The open triangle for  $V_{pL} = -90$  mV data denotes a zero-bias Kondo peak.

the opposing sides of the quasi-one-dimensional QW (having two to three conduction channels for the gate voltage conditions explored) with a small relative distance along the wire direction.<sup>15,16</sup> Hence, the ferromagnetic coupling may be realized, and a relatively large interaction strength is expected. If this is the case, the localized spin in one QD is ferromagnetically locked by the remote spin in the other QD, and the Kondo effect is suppressed. However, this RKKY mechanism is inseparable from the Fano-Kondo-modulated density of states scenario described above, and presumably both mechanisms are in action.

By applying magnetic field perpendicular to the 2DEG plane, one can reduce the tunnel coupling without the electrostatic energy shift. Figure 3(b) shows the same data as in Fig. 3(a) except that  $B = 0.15$  T. In this case, conductance modulation by  $V_{pL}$  is absent and the overall conductance is enhanced compared to Fig. 3(a). This is because the left QD is decoupled by magnetic field and the Fano (-Kondo) effect disappears. In fact, the Kondo effect is recovered within the whole Kondo valley irrespective of  $N_L$ . When much stronger

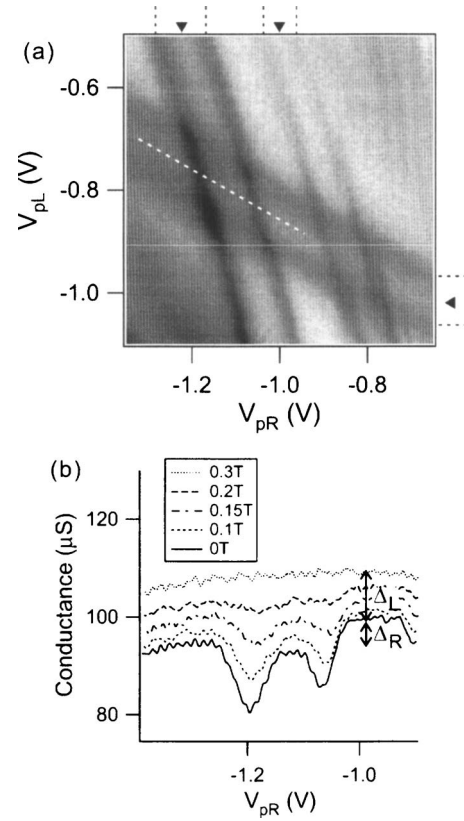


FIG. 4. (a) Gray-scale of plot of the conductance through the QW as a function of  $V_{pL}$  and  $V_{pR}$  with  $V_{sL} = -1.15$  V,  $V_{sR} = -1.25$  V,  $V_{dL} = V_{dR} = -0.5$  V, and  $V_{mL} = V_{mR} = -0.4$  V. Black corresponds to  $2e^2/h$  ( $77 \mu S$ ) and white to  $3e^2/h$  ( $116 \mu S$ ). Black dotted lines and solid triangles on the axes denote Fano resonances and odd electron number regions, respectively. (b) Magnetic field dependence of the QW conductance profile taken along the white dotted line in (a) with constant  $N_L$  ( $V_{pL}$  and  $V_{pR}$  are simultaneously swept).  $\Delta_R$  and  $\Delta_L$  denote the conductance suppression due to the Fano-Kondo effect involving the right QD and the left QD, respectively.

magnetic field is applied ( $\geq 1$  T), the Kondo effect is eventually suppressed because of the Zeeman splitting and the reduced dot-lead tunnel coupling, as Fig. 1(c) suggests. These two different magnetic field scales indicate that the dot-lead coupling is more robust than the dot-wire side coupling.

Finally, we change the experimental setup and measure the current through the QW. Figure 4(a) shows gray-scale plot of the QW conductance as a function of  $V_{pL}$  and  $V_{pR}$ . The exit of both QDs are pinched off. Four (two) clear Fano resonances are observed for the right (left) QD indicated by black dotted lines on the axes. Surprisingly, the period of these Fano resonances ( $\sim 100$  mV) is much larger than the typical resonance period ( $< 30$  mV) discussed so far. Actually, such small period resonances are also found in Fig. 4(a) at  $V_{pR} > -0.9$  V. Therefore, we ascribe the large period resonances to smaller QDs (having larger charging energy) which are formed after the original QDs are pinched off. This may be related to our specific gate electrode geometry where, unlike conventional design, the plunger gate electrodes are not recessed with respect to the exit gate electrodes to which  $V_{dL}$  and  $V_{dR}$  are applied. The electrostatic coupling between

the original QD and the smaller QD on the right side is observed as a honeycomblike pattern at  $V_{\text{pR}} \approx -0.8$  V, as is commonly observed in the stability diagram of a normal double dot.<sup>28</sup> The different slopes of the resonance lines between the smaller QDs and the original ones reflect the fact that the smaller QDs are located closer to the center than the original ones and have a larger capacitive coupling to the plunger gate on the opposite side.

Let us now focus on the features originating from the smaller QDs. Each resonance line is almost straight and does not show the honeycomb distortion, indicating that the change in  $N_L$  ( $N_R$ ) by one has negligible influence on the electrostatic energy of the right (left) QD because of the interceding QW. The conductance at the odd  $N$  regions marked with solid triangles are suppressed due to the Fano-Kondo effect. In particular, the conductance is minimum when both  $N_L$  and  $N_R$  are odd because of the double Fano-Kondo suppression.<sup>16,29</sup>

Figure 4(b) shows the magnetic field dependence of the conductance profile taken along the white dotted line in Fig. 4(a) with constant odd  $N_L$ . In the  $B=0$  T trace, there are two dips at  $V_{\text{pR}}=-1.05$  V and at  $V_{\text{pR}}=-1.2$  V due to the Fano resonance between the right QD and the QW. The conductance between the dips (odd  $N_R$ ) are suppressed compared with the outer regions (even  $N_R$ ) due to the Fano-Kondo effect. As magnetic field increases, tunnel coupling between the QD and the QW is reduced. Then, the Fano resonances and the Fano-Kondo effect are suppressed and the overall conductance gradually increases. By comparing the trace at  $B=0.3$  T, where all the features are lost, and that at  $B=0$  T, the suppressed conductance due to the Fano-Kondo effect involving the right (left) dot,  $\Delta_R$  ( $\Delta_L$ ), is estimated to be  $5 \mu\text{S}$  ( $10 \mu\text{S}$ ) at the center of the double-suppression region, as shown in Fig. 4(b).

#### IV. SUMMARY

We have performed transport measurement on the double QD-QW coupled system and demonstrated nonlocal control of the Kondo effect in one QD by manipulating the spin states of the other. The Kondo temperature in one QD may be modulated via the local density of states modulation in the QW due to the Fano-Kondo antiresonance involving the other QD. As another mechanism, the RKKY interaction between the two QDs is considered. We have also observed the double Fano-Kondo antiresonance in the conductance of the QW when both QDs have odd electrons. We have found that all the features measured in two different setups are dimin-

ished by the application of a magnetic field perpendicular to the 2DEG, which reduces the tunnel couplings between QDs and QW.

#### ACKNOWLEDGMENT

This work is financially supported by Grant-in-Aid for Scientific Research from the Japan Society for the Promotion of Science.

<sup>1</sup>L. I. Glazman and M. E. Raikh, JETP Lett. **47**, 452 (1988).

<sup>2</sup>T. K. Ng and P. A. Lee, Phys. Rev. Lett. **61**, 1768 (1988).

<sup>3</sup>D. Goldhaber-Gordon, H. Shtrikman, D. Mahalu, D. Abusch-Magder, U. Meirav, and M. A. Kastner, Nature **391**, 156 (1998).

<sup>4</sup>S. M. Cronenwett, T. H. Oosterkamp, and L. P. Kouwenhoven, Science **281**, 540 (1998).

<sup>5</sup>J. Schmid, J. Weis, K. Eberl, and K. von Klitzing, Physica B **256–258**, 182 (1998).

<sup>6</sup>W. G. van der Wiel, S. De Franceschi, T. Fujisawa, J. M. Elzerman, S. Tarucha, and L. P. Kouwenhoven, Science **289**, 2105 (2000).

<sup>7</sup>A. C. Johnson, C. M. Marcus, M. P. Hanson, and A. C. Gossard, Phys. Rev. Lett. **93**, 106803 (2004).

<sup>8</sup>K. Kobayashi, H. Aikawa, S. Katsumoto, and Y. Iye, Phys. Rev. Lett. **88**, 256806 (2002).

<sup>9</sup>K. Kobayashi, H. Aikawa, A. Sano, S. Katsumoto, and Y. Iye, Phys. Rev. B **70**, 035319 (2004).

<sup>10</sup>K. Kang, S. Y. Cho, J. J. Kim, and S. C. Shin, Phys. Rev. B **63**, 113304 (2001).

<sup>11</sup>M. A. Davidovich, E. V. Anda, C. A. Busser, and G. Chiappe, Phys. Rev. B **65**, 233310 (2002).

<sup>12</sup>M. E. Torio, K. Hallberg, A. H. Ceccatto, and C. R. Proetto, Phys. Rev. B **65**, 085302 (2002).

<sup>13</sup>I. Maruyama, N. Shibata, and K. Ueda, J. Phys. Soc. Jpn. **73**, 3239 (2004).

<sup>14</sup>M. Sato, H. Aikawa, K. Kobayashi, S. Katsumoto, and Y. Iye, Phys. Rev. Lett. **95**, 066801 (2005).

<sup>15</sup>H. Tamura, K. Shiraiishi, and H. Takayanagi, Jpn. J. Appl. Phys. **43**, L691 (2004).

<sup>16</sup>H. Tamura and L. Glazman, Phys. Rev. B **72**, 121308(R) (2005).

<sup>17</sup>N. J. Craig, J. M. Taylor, E. A. Lester, C. M. Marcus, M. P. Hanson, and A. C. Gossard, Science **304**, 565 (2004).

<sup>18</sup>P. Simon, Phys. Rev. B **71**, 155319 (2005).

<sup>19</sup>P. Simon, R. Lopez, and Y. Oreg, Phys. Rev. Lett. **94**, 086602 (2005).

<sup>20</sup>M. G. Vavilov and L. I. Glazman, Phys. Rev. Lett. **94**, 086805 (2005).

<sup>21</sup>M. Stopa, W. G. van der Wiel, S. De Franceschi, S. Tarucha, and L. P. Kouwenhoven, Phys. Rev. Lett. **91**, 046601 (2003).

<sup>22</sup>A. Richter, M. Yamaguchi, T. Akazaki, H. Tamura, and H. Takayanagi, Jpn. J. Appl. Phys., Part 1 **43**, 7144 (2004).

<sup>23</sup>S. Sasaki *et al.*, Phys. Rev. B **73**, 161303(R) (2006).

<sup>24</sup>J. M. Elzerman, R. Hanson, J. S. Greidanus, L. H. Willem van Beveren, S. De Franceschi, L. M. K. Vandersypen, S. Tarucha, and L. P. Kouwenhoven, Phys. Rev. B **67**, 161308(R) (2003).

<sup>25</sup>R. Hanson, B. Witkamp, L. M. K. Vandersypen, L. H. Willem van Beveren, J. M. Elzerman, and L. P. Kouwenhoven, Phys. Rev. Lett. **91**, 196802 (2003).

<sup>26</sup>J. M. Elzerman, R. Hanson, L. H. Willem van Beveren, B. Witkamp, L. M. K. Vandersypen, and L. P. Kouwenhoven, Nature **430**, 431 (2004).

<sup>27</sup>D. L. Cox and A. Zawadowski, Adv. Phys. **47**, 599 (1998).

<sup>28</sup>W. G. van der Wiel, S. De Franceschi, J. M. Elzerman, T. Fujisawa, S. Tarucha, and L. P. Kouwenhoven, Rev. Mod. Phys. **75**, 1 (2003).

<sup>29</sup>P. Stefanski, Solid State Commun. **128**, 29 (2003).